Hindawi Publishing Corporation
Journal of Nanomaterials
Volume 2012, Article ID 724857, 10 pages
doi:10.1155/2012/724857

Research Article

Self-Assembling Peptide Nanofiber Scaffold Enhanced with RhoA Inhibitor CT04 Improves Axonal Regrowth in the Transected Spinal Cord

Weiwei Zhang,[1] Xiaoduo Zhan,[1] Mingyong Gao,[2] Audra D. Hamilton,[3] Zhongying Liu,[1] Yanwen Jiang,[1] Huanxing Su,[2] Xiang Dai,[1] Bin He,[4] Xiaoning Kang,[1] Yuanshan Zeng,[4] Wutian Wu,[2,5,6] and Jiasong Guo[1]

[1] *Department of Histology and Embryology, Southern Medical University, Guangzhou 510515, China*
[2] *Department of Anatomy, Li Ka Shing Faculty of Medicine, The University of Hong Kong, Pokfulam, Hong Kong*
[3] *Department of Neurology, Vanderbilt University, Nashville, TN 37232, USA*
[4] *Department of Histology and Embryology, Sun Yat-Sen University, Guangzhou 510080, China*
[5] *Joint Laboratory for Brain Function and Health (BFAH), Jinan University and The University of Hong Kong, Guangzhou 510630, China*
[6] *State Key Laboratory of Brain and Cognitive Sciences, The University of Hong Kong, Pokfulam, Hong Kong*

Correspondence should be addressed to Wutian Wu, wtwu@hkucc.hku.hk and Jiasong Guo, jiasongguo@yahoo.com.cn

Received 15 December 2011; Revised 14 March 2012; Accepted 18 March 2012

Academic Editor: Xiaoyi Wu

The present study was designed to explore the therapeutic potential of self-assembling peptide nanofiber scaffold (SAPNS) delivered RhoA inhibitor to ameliorate the hostile microenvironment of injured spinal cord for axonal regeneration. After a transection was applied to the thoracic spinal cord of mice, the combination of SAPNS and CT04 (a cell permeable RhoA inhibitor), single SAPNS with vehicle, or saline was transplanted into the lesion cavity. Results showed that SAPNS+CT04 implants achieved the best therapeutic outcomes among treatment groups. The novel combination not only reconstructed the injured nerve gap but also elicited significant axonal regeneration and motor functional recovery. Additionally, the combination also effectively reduced the apoptosis and infiltration of activated macrophages in the injured spinal cord. Collectively, the present study demonstrated that SAPNS-based delivery of RhoA inhibitor CT04 presented a highly potential therapeutic strategy for spinal cord injury with reknitting lesion gap, attenuating secondary injury, and improving axonal regrowth.

1. Introduction

Spinal cord injury (SCI) causes a permanent neurological disability. Axonal regeneration is very limited in the adult after SCI with no satisfactory treatment available to date. Various regeneration inhibitors derived from resultant glial scar and myelin debris have been regarded as main obstacles to impede axonal regrowth [1] such as chondroitin sulfate proteoglycans (CSPGs) from glial scar [2], Nogo, myelin-associated glycoprotein (MAG), and oligodendrocyte-myelin glycoprotein (OMgp) derived from myelin [3]. Blocking these inhibitors has been tested to improve neural regeneration after SCI. An increasing body of promising data has been reported, which includes the administration of degrading enzymes [4], neutralizing antibodies [5], and Nogo-66 receptor antagonist peptide [6]. However, blocking a single molecular target may not be sufficient to achieve satisfactory axonal regeneration as extensive as molecular cascades in terms of regrowth inhibition during the pathophysiological procedures involved after SCI. Most of axonal growth-suppressing factors are intracellularly mediated via activation of a small GTP-binding protein RhoA [7–9], which implicates that the inactivating of RhoA signaling would represent a novel strategy to improve the neural regeneration after SCI [10–13].

However, the way to introduce the RhoA inhibitors into the injured spinal cord still remains a challenge due to the multiple inherent limitations of the traditional delivery approaches [14]. For example, it is only effective when high

dosage of inhibitors has been administrated by oral uptake [9] or intraperitoneal injection [9, 15], since the inhibitors are difficult to be concentrated in the target tissue naturally. Moreover, such kind of delivery of the inhibitors with high dosage may result in unexpected side effects to the other systems in vivo. As to the intrathecal injection [16, 17], it would be most likely accompanied with unnecessary side injury to the healthy cord parenchyma during manipulation. Recently, fibrin sealant has been reported to act as delivery matrice of such inhibitor-antagonists for the treatment of SCI [14, 18] in terms of local delivery, which would be a promising strategy to overcome the main limitations of traditional methods.

In the present study, self-assembling peptide nanofiber scaf-fold (SAPNS) based local delivery of RhoA inhibitor was applied for the repair of injured spinal cord. As our previous studies show, the SAPNS has multiple regeneration-facilitating properties to improve the recovery of the injured spinal cord and brain [19, 20]. More interesting, SAPNS has been showed highly potential for controlled drug release in various in vitro or in vivo studies [21–26]. Therefore, we transplanted SAPNS mixed with a cell permeable RhoA inhibitor into the lesion sites after acute SCI in adult animal subjects. It is hypothesized that this novel combination might overcome two of the main obstacles for SCI simultaneously. One obstacle is reconstructing the gap in the injured spinal cord and providing regrowth-promoting scaffold reducing the physical obstacles after injury, as SAPNS is capable of filling the cavities and alleviating glial scarring after SCI [19, 20]. The other lies in that RhoA inhibitor released from the combination implants may exert inactivation of RhoA to ameliorate the hostile microenvironment perilesion which would be greatly conducive for axonal regrowth.

2. Materials and Methods

2.1. Materials. In the present study, CT04 (Cytoskeleton, Denver, CO), a cell permeable Rho inhibitor, was used to inhibit activities of GTPase RhoA. The active site of CT04 is the exoenzyme C3 transferase from clostridium botulinum. C3 transferase specifically inhibits RhoA by ADP-ribosylation on asparagine 41 in the effector-binding domain of the GTPase [27]. The lyophilized powder of CT04 was reconstituted with sterile 50% glycerol aqueous solution to yield a concentration of 1 mg/mL and stored at −20°C for further administration.

RADA16-I peptides (BD Biosciences, Cambridge, MA), a type I SAPNS [28], were used serving as biomaterial implants which were incorporated with CT04 before transplantation. Ten to thirty minutes before implantation, 2 μL of reconstituted CT04 solution was quickly mixed up with 13 μL SAPNS in a culture dish. Then, 1 mL DMEM/F12 culture medium (Gibco) was gently added to trigger gelatinization of the mixture. Additionally, 2 μL sterile 50% glycerol aqueous solution without CT04 was mixed with 13 μL SAPNS following gelatinization to act as a control. In order to assess the release of chemical from SAPNS gel in vivo, a mixture of SAPNS (13 μL) and 2% fluorescent dye Dextran (2 μL, molecular weight: 10 k dalton) was implanted into 2 mice.

2.2. Surgical Procedures. Adult wild-type female Kunming mice (74 in total) weighing 25 to 35 g (from the Experimental Animal Center of Southern Medical University) were used in this study, which were divided to 4 groups randomly: sham surgery ($n = 12$), saline control ($n = 20$), SAPNS + glycerol vehicle ($n = 20$), and SAPNS+CT04 implant ($n = 20$). The remaining 2 mice were treated with the mixture of SAPNS and Dextran. The guidelines for Animal Care and Use of Southern Medical University were strictly followed during the surgery procedures. Briefly, the mice were intraperitoneally injected with pentobarbital sodium for anesthesia (30 mg/kg body weight). After toe reflection disappeared, a dorsal laminectomy was carried out to expose the T9-10 spinal cord. A full transection at the T9 cord level was made, and separated cord tissue was removed to produce 1 mm long gap. With the aid of a surgical microscope, the various prepared SAPNS scaffold combinations were implanted into the lesion cavity (Figures 1(c) and 1(d)). For the negative control, 15 μL saline was filled into the lesion cavity (Figure 1(b)). In the sham surgery, group mice received laminectomy without cord transection (Figure 1(a)). The bladder was emptied manually twice a day until urinary reflex was reestablished in the transection groups.

2.3. Retrograde Tracing. Twelve weeks after treatment, 5 mice of each group were subjected to the retrograde tracing with FluoroGold (FG, Sigma) labeling. A dorsal laminectomy was carried out to expose the T11-T12 spinal cord. One μL of 1% FG was microinjected into the spinal cord at two different sites with each being 6 mm caudal to the transected site and 1 mm in depth to the dorsal surface by a Hamilton syringe with 30-gauge needle. The injection needle was slowly withdrawn after leaving in place for an additional 5 minutes. The operating field was cleaned with saline, and 2 μL of SAPNS was dropped onto the surface of the injected hole to prevent tracer leakage. Animals were allowed to survive for another 7 d for tracer transportation before they were sacrificed.

2.4. Tissue Preparation and Histological Analysis. At the designed time point, the animal subjects were perfused transcardially with 4% paraformaldehyde in 0.1 M PBS (pH 7.4) after an overdose administration of pentobarbital. The spinal cord and brain were subsequently postfixed overnight, then the tissues were cryoprotected in 30% sucrose for additional 72 h at 4°C and embedded in optimum cutting temperature (OCT) medium for sectioning. One cm of the spinal cord centered at the injury site was horizontally sectioned with a cryostat (Leica) for 15 μm thick successive sections. Brain tissues with red nuclei (RN) or SMC were cut coronarily with 30 μm in thickness. All sections were mounted onto gelatin-subbed slides and stored at −20°C for the further use.

For immunostaining, the frozen slides were washed with PBS for 10 min and blocked with 1% BSA and 10% normal goat serum in 0.3% Triton X-100 PBS for 1 h at room

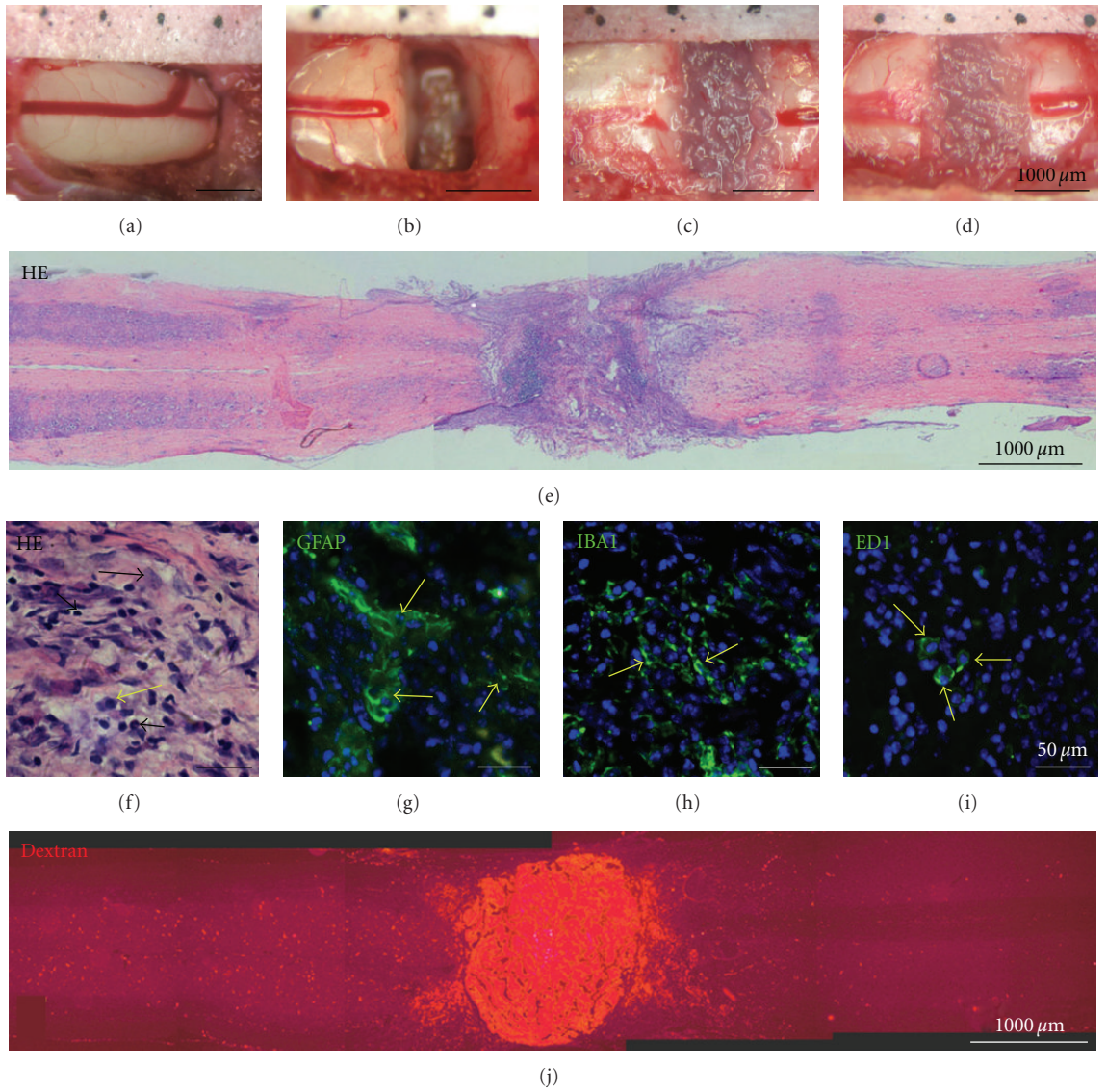

Figure 1: The implants of various SAPNS reconstructed the injured spinal cord. (a–d) Macroscopic observations of lesion sites immediately after surgery. (a) Sham surgery; (b) saline group; (c) SAPNS with vehicle group; (d) SAPNS+CT04 combination group. (e) HE staining shows the lesion area was reconstructed 12 weeks after SAPNS transplanted. (f) HE staining shows various cells in the grafted scaffold, which include fibroblast (black arrow), macrophage (yellow arrow), and lymphocyte (arrow head). (g–i) Immunostaining shows the GFAP-positive astrocytes (g), IBA1 positive microglias (h) and ED1 positive macrophages (i) in the grafted scaffold. (j) shows the Dextran, a red fluorescent dye, was partially diffused from the mixture of SAPNS and Dextran at 7 days after transplantation. Scale bar is 1000 μm for (a–e) and (j), 50 μm for (f-g).

temperature (RT). The following primary antibodies were applied for incubation overnight at 4°C: rabbit anti-RhoA (1 : 200, Santa Cruz), mouse anti-NF200 (1 : 400; Sigma), and mouse anti-ED1 (1 : 1000, Serotec) mouse anti-CS56 (1 : 400; Sigma), rabbit anti-GFAP(1 : 1000, Millipore), rabbit anti-IBA1 (1 : 1000; Osaka). Subsequently, the slides were washed in PBS three times and incubated with fluorescent Alexa 488 or 568 conjugated goat anti-mouse or goat anti-rabbit secondary antibodies (1 : 400; Molecular Probes) for 2 h at room temperature. The slides were cover slipped with mounting medium (Dako) containing DAPI to counter stain the nuclei.

For detection of the FG tracing, spinal cord and brain sections from FG-labeled animal subjects were cover slipped with mounting medium (Dako) containing DAPI to counter stain the nuclei after washing with PBS three times (5 minutes each) and then observed by fluorescent microscope.

2.5. Fluorescent TUNEL Staining. The fluorescent terminal deoxynucleotidyl transferase biotin-dUTP nick end labeling (TUNEL) assay kit (Roche, Mannheim, Germany) was used to detect in situ DNA fragmentation as described in the kit's instructions. Briefly, the slides were washed twice in PBS and

soaked in 0.5% Triton-100 (prepared in PBS) at RT for 15 minutes then washed twice in PBS again before incubating with TUNEL reaction mixture at 37°C for 90 minutes. The slides were coverslipped with mounting medium after counterstaining the nuclei with DAPI.

2.6. Quantification of Regenerated Axons, FG-Labeled Neurons, ED1-Positive Macrophages, and TUNEL-Positive Apoptosis Cells. To quantify the density of NF-200 positive axons that regenerated into the graft, a modified approach derived from the previous reports [19, 29] was utilized. Briefly, the NF-200 positive axons in the graft were visualized and quantified under a fluorescent microscope. Every one of six spinal cord sections in serial was selected to perform the quantification. A line perpendicular to the longitudinal axis was superimposed onto the centre of the graft, and axons intercepted with the superimposed line were counted. The total number of axons obtained from all selected sections was defined as the number of axons of each animal.

The sections selected as described above were also used to quantify the FG-labeled neurons, ED1-positive macrophages, or TUNEL-positive apoptosis cells. All the targeted cells from 6 mm rostral to the lesion site to the edge of lesion site were counted. The total number obtained from all sections was defined as the number of each animal.

2.7. Electrophysiologic Analysis. Twelve weeks after treatment, the animal subjects were anesthetized and stereotaxically fixed. Following the exposure of bilateral sciatic nerves and sensory-motor cortex (SMC), the electrodes of BL- 420E Data Acquisition and Analysis System for Life Science (Taimeng, Chengdu, China) were connected to the sciatic nerve and SMC. Guided by the instructions of the system menu, the latency and amplitude of the cortical motor evoked potential (CMEP) were measured and recorded for the further analysis [30].

2.8. Behavioral Testing. The motor functional recovery of injured animal subjects was assessed with the Basso Mouse Scale (BMS) approach [31] at 1, 6, and 12 weeks respectively posttreatment. The BMS is a ten-point locomotor rating scale for assessment of motor functional recovery ranging from 0 (=complete hind-limb paralysis) to 9 (=normal locomotion). Based on observation of hind-limb movements in an open field during a 4-minute interval at each time point, the involved behavioral performance of animal subjects was scored by two investigators who were blind to the experimental groups.

2.9. Statistical Analysis. Statistical comparisons were performed with analysis of variance (ANOVA) with repeated measures or by Student paired t-test for paired observations. P values of 0.05 or less were considered as statistical significantly different.

3. Results and Discussion

3.1. The Implants of Various SAPNS Reconstructed the Injured Spinal Cord. A significant gap was developed in the lesion site in the saline group. In contrast, the initial lesion gap was bridged well by the grafted SAPNS implants with or without CT04 incorporation. Of note, the implants integrated smoothly with the surrounding host tissue without obvious cavities or gaps occurring between the implants and host (Figure 1(e)). In the subjects of 12 weeks after transplantation, we found lots of cells migrated into the graft. The majority of the cells were fibroblasts, which mainly clustered in the center of the lesion area and formed collagen fibers. There were some lymphocytes, macrophages, astrocytes, and microglias scattered among the fibroblasts (Figures 1(f), 1(g), 1(h), 1(i)). As it is well known, the cavity or cysts formation developed in the injured spinal cord remains the major pathological obstacle to the axonal regrowth due to the anatomical disconnection [32]. Therefore, it is critical and fundamental to bridge and reconstruct the lesion gap or formed cyst after SCI. The grafted scaffold and the extracellular matrix excreted from the migrated cells should provide the essential physical support and guidance for the regenerating axons to extend across the lesion site. In the present study, a lot of neurofilament (NF) positive axons were found to regrow into the grafted SAPNS implants in the injured spinal cord (Figure 2). With FG-retrograde tracing, a number of FG-labeled neurons were detected in the rostral spinal cord, RN, and inner pyramidal layer of SMC (Figure 3) across the lesion sites.

3.2. SAPNS Delivery of CT04 Significantly Improved the Axonal Regrowth. As a novel nanobiomaterial, SAPNS has been demonstrated to have multiple benefits to the tissue repair over the other biomaterials currently, such as minimal risk of carrying biological pathogens or contaminants, a true 3-dimensional environment constructed for cell growth and migration, minimal cytotoxicity to the host, no apparent immune response, easy conformity to the various shape of lesion cavities, and immediate haemostatic and controlled drug release properties [19–26, 33, 34]. In this study, we used dextran, a fluorescent dye, to show whether SAPNS can serve as a platform for controlled release in the injured spinal cord. Seven days after the transplantation of the SAPNS incorporated with Dextran, some of the fluorescence was observed to diffuse into the surrounding host cord from the SAPNS, while the implant still retained high fluorescent signal (Figure 1(j)). The fluorescent dye used here confirmed that the chemicals released were from the SAPNS implants, which indicated that SAPNS can effectively serve as a platform for further controlled release of exogenous therapeutic moleculars of interest that have been introduced into the injured spinal cord, like its application is reported in the other tissues [20, 21].

Compared with the traditional methods for drug administration, the use SAPNS to deliver RhoA inhibitor to injured spinal cord has multiple benefits. The drug is easy to be concentrated in the lesion area, so it can increase the efficiency on the target while decrease the side effects to other

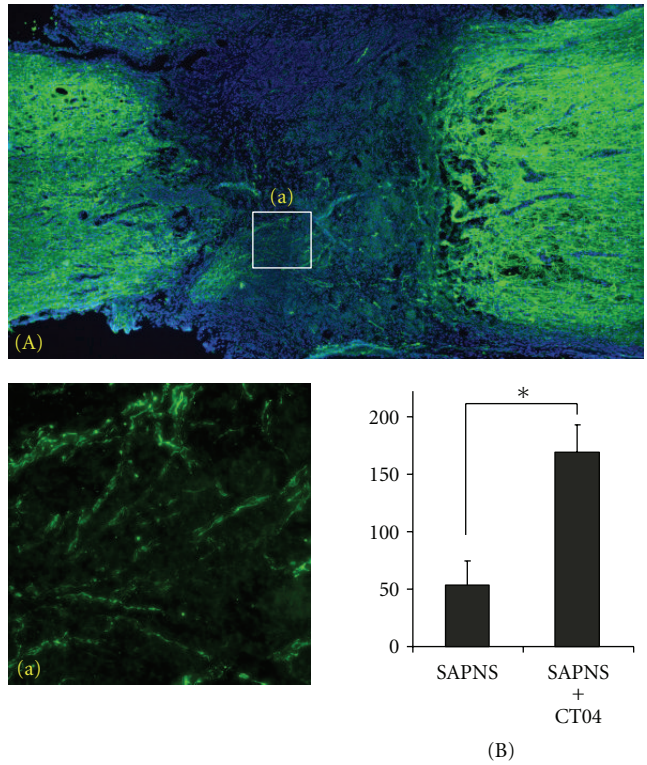

Figure 2: Axonal regrowth in the SAPNS treatment groups. (A) Neurofilament (NF) immunohistochemistry staining shows numbers of NF-positive axons regenerated into the lesion sites with SAPNS+CT04 treatment (the NF immunoreactivities are in green). The blue area is the distribution of counterstained DAPI to show the gross structure of the injured spinal cord. (a) The high power magnification corresponding to the box area of (A) shows the NF positive axons in the center of the lesion area. (B) Quantification of the NF positive axons in the center of the lesion area showed the axonal regrowth was significantly improved by the SAPNS+CT04 implants compared to the SAPNS group ($^*P < 0.05$).

tissue.The dosage can be reduced significantly compared to oral uptake or injection. By this method, reconstructing the lesion site and administrating RhoA inhibitor can be achieved in a simple step.

In the present study, immunohistochemical staining revealed that NF-positive axons grew into the lesion area treated with SAPNS grafts. Compared with SAPNS implant with vehicle alone, the regenerated axons in the implants of SAPNS enhanced with CT04 incorporation were increased significantly (Figure 2). Furthermore, the FG retrograde labeling experiment demonstrated that, in the SAPNS plus CT04 group, a large number of neurons, rostral to the transected sites, were labeled with FG (Figure 3(J), (j)). The number of FG-labeled neurons was significantly higher in SAPNS+CT04 group than that of SAPNS with vehicle (Figure 3(M)). The FG-labeled neurons also appeared in most of RN and SMC sections (Figure 3(K), (L)). Contrastingly, no FG-labeled neurons were found in the brain and cord tissue rostral to the transected sites in the saline group (Figure 3(D), (d), (E), and (F)). Notably, a few of FG-labeled neurons were found in the rostral spinal cord in control SAPNS groups (Figure 3(G), (g)) with an occasional one or two FG-labeled neurons in some of the RN and SMC sections (Figure 3(H), (I)). In the sham surgery subjects, a lot of FG-labeled neurons were found in the spinal cord (Figure 3(A), (a)), RN (Figure 3(B)) and inner pyramidal layer of SMC (Figure 3(C)). It is evident that the FG-labeled neurons represented the rostral neuronal populations regenerating their axons across the lesion sites and reached the caudal side.

3.3. The Functional Recovery Was Enhanced by the Implants. Electrophysiological results showed that the CMEP was hardly detectable in the saline-treated mice, and the amplitude of CMEP detected was extremely low and the latency appeared much longer than that of the sham surgery subjects. In contrast, the CMEP of SAPNS+CT04 group was recovered significantly better than that of SAPNS alone and saline control (Figure 4(a)–(c)). Similarly, among the treatment groups, the motor functional recovery assessed by BMS assay also showed that the recovery scoring after SCI was highest in the group treated with SAPNS+CT04 followed by the SAPNS group. The saline group presented very limited recovery (Figure 4(d)).

3.4. The Inflammation, Apoptosis, and Glial Scarring Were Alleviated by the Implants. To determine whether inflammation and apoptosis are regulated by the SAPNS+CT04 implant or SAPNS with vehicle, immunostaining with ED1 antibody or in situ TUNEL was performed 7 days after

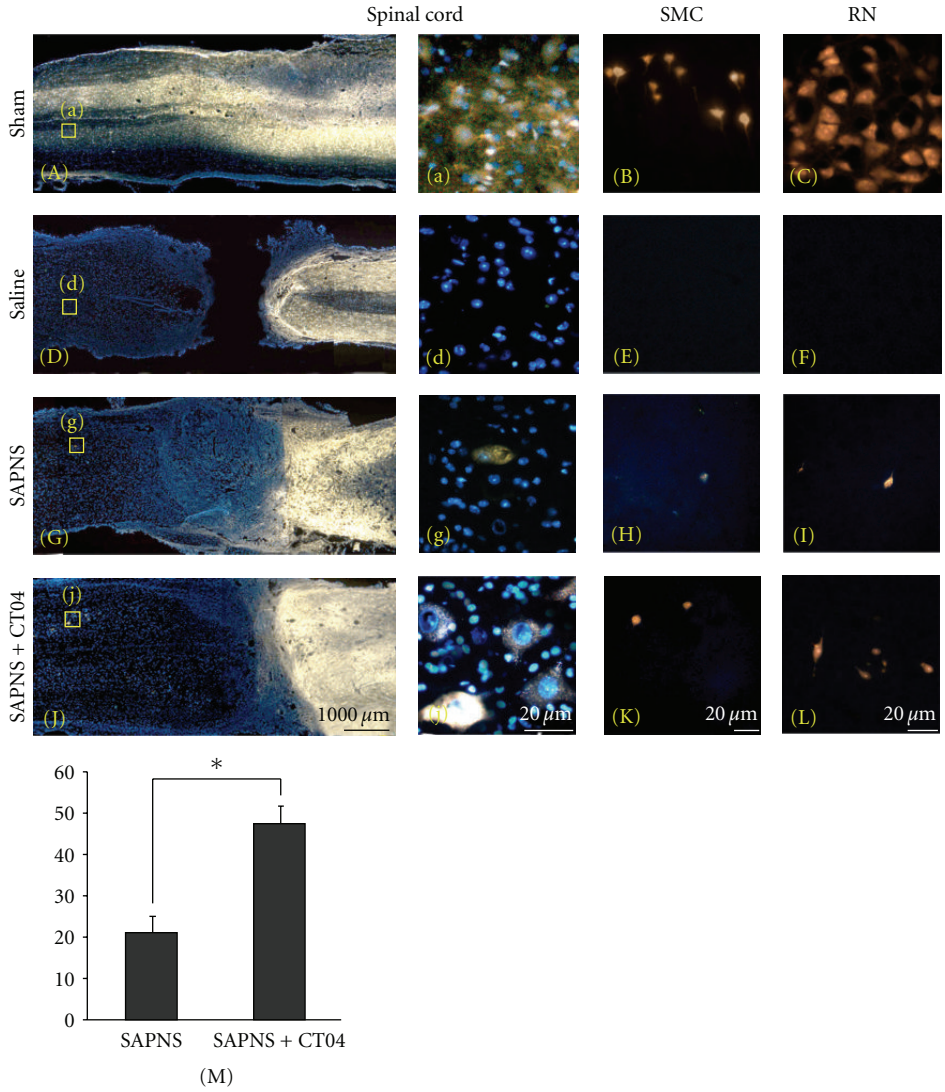

Figure 3: Retrograde labeling of FG after SCI. (A, D, G, and J) shows the overviews of the FG-labeled spinal cord 13 weeks after treatments (rostral is to the left). (a, d, g, and j) are higher power magnification corresponding to boxed areas in (A, D, G, and J), respectively. The FG labeled neurons are in yellow. (B, E, H, K) and (C, F, I, L) show the FG-labeled neurons that appeared in the sensor-motor cortex (SMC) and red nuclei (RN) in different groups. (M) shows the quantification of FG-labeled neurons in the rostral spinal cord, indicating significant difference between SAPNS+CT04 and SAPNS with vehicle groups at 13 wks ($^*P < 0.05$).

treatment. There were no ED1 or TUNEL positive cells in the sham surgery group (Figure 5(a), (e)), but a large number of ED1 or TUNEL positive cells appeared in the saline-treated group (Figure 5(b), (f)). Most of the positive cells surround the injured area. The number of both ED1 and TUNEL positive cells were decreased with SAPNS treatment (Figure 5(c), (g)), and minimum positive staining was detected in the SAPNS+CT04 group (Figure 5(d), (h)). Statistical analysis showed there were significant differences among groups (Figure 5(i), (j)). ED1 is a marker of macrophages. Macrophage infiltration is a main index of inflammation after SCI. TUNEL assay is a routine method to detect apoptosis cells. Moreover, we did immunostaining with CS56 antibody to detect the chondroitin sulfate proteoglycans (CSPGs, which are main components of the glial scar in the injured spinal cord). Results showed the CSPG expression decreased in the SANPS+CT04 treated subjects compared with that of SAPNS with vehicle (Figure 5(k)–(n)). Therefore, these results indicated that SAPNS+CT04 combination could significantly alleviate the inflammation, apoptosis, and glial scarring.

Not surprisingly, the strong RhoA immunoreactivities were detected in all SCI groups, but there was not an obvious difference among the three SCI groups (Figure 5(p)–(r)). Additionally, the RhoA immunoreactivity was not detected in the sham surgery group (Figure 5(o)). This observation is parallel to the previous report [8].

Axonal regrowth requires rearrangement of the cytoskeleton at the growth cone. The Rho family of small GTPases serves as "molecular switches" to regulate the cytoskeletal

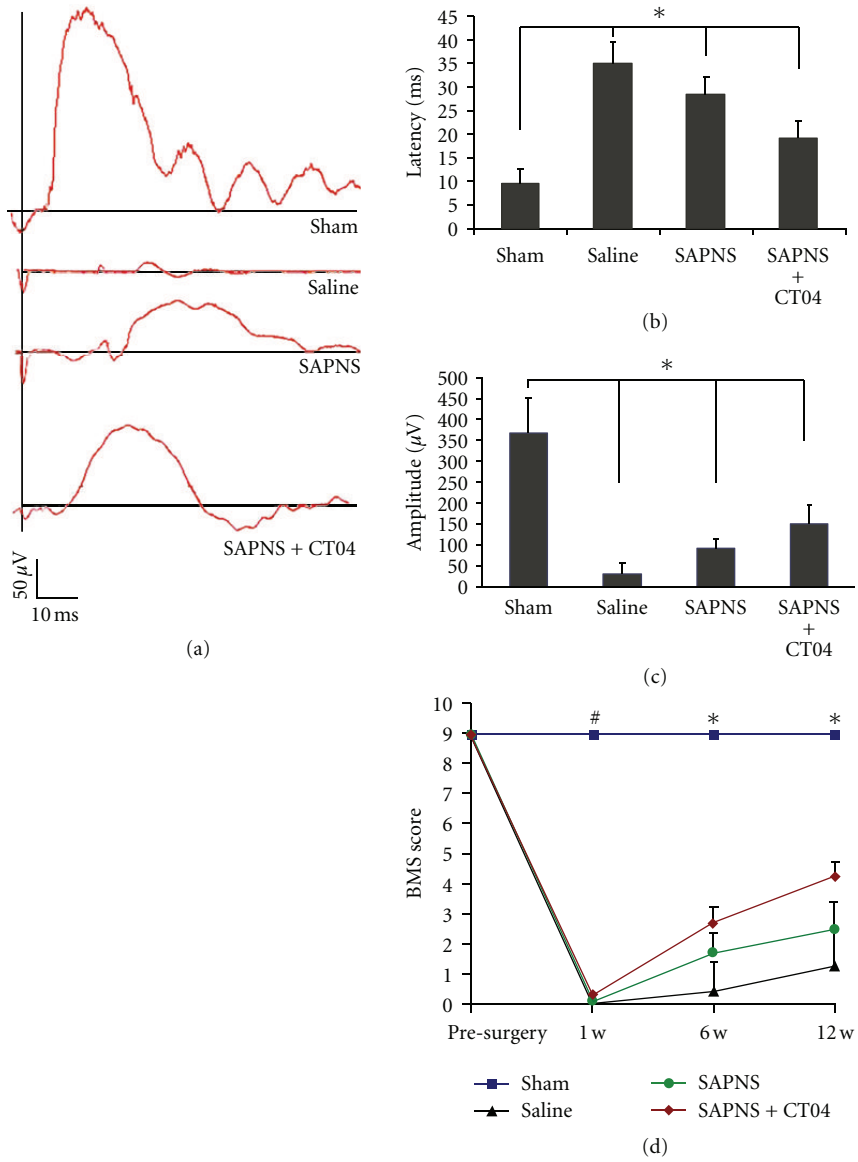

Figure 4: Electrophysiological and motor behavioral assessments 12 wks after treatments. (a) shows the representative record of cortical motor evoked potential (CMEP) from 4 groups at 12 weeks after treatment; (b) and (c) show the statistics data of latencies and amplitudes of CMEP indicating significant differences among 4 groups at 12 wks ($^{*}P < 0.05$). (d) shows the BMS score at 1, 6, and 12 weeks after surgery respectively. At 1 week, only sham surgery group has significant difference with other groups ($^{\#}P < 0.05$). At 6 weeks and 12 weeks, significant differences were shown among 4 groups ($^{*}P < 0.05$).

rearrangements [35]. They are able to remodel the actin cytoskeleton and control actin polymerization, branching, and bundling. Different members of Rho-family have different functions on axonal regrowth, such as Rac1 and Cdc42 promote growth cone advance, while RhoA inhibits axon growth or induces retraction through growth cone collapse [36]. Trauma triggers RhoA activation in injured spinal cord by upregulation of RhoA protein expression [8, 37]. It was also confirmed in our present results (Figure 5(o)–(r)) that the upregulated RhoA plays a crucial role in the failure of axonal regrowth after SCI. It initiates not only growth cone collapse, but also macrophage infiltration [38] and apoptosis [18], which represent the main aspects of the secondary injury after SCI that are believed to be the key therapeutic targets for the treatment of SCI.

4. Conclusion

In the present study, a novel combination of SAPNS and CT04 was implanted into the adult injured spinal cord. SAPNS implants effectively reconstructed the lesion gap and partially induced axonal regrowth and functional recovery by the combinatorial delivery. As a new kind of cell

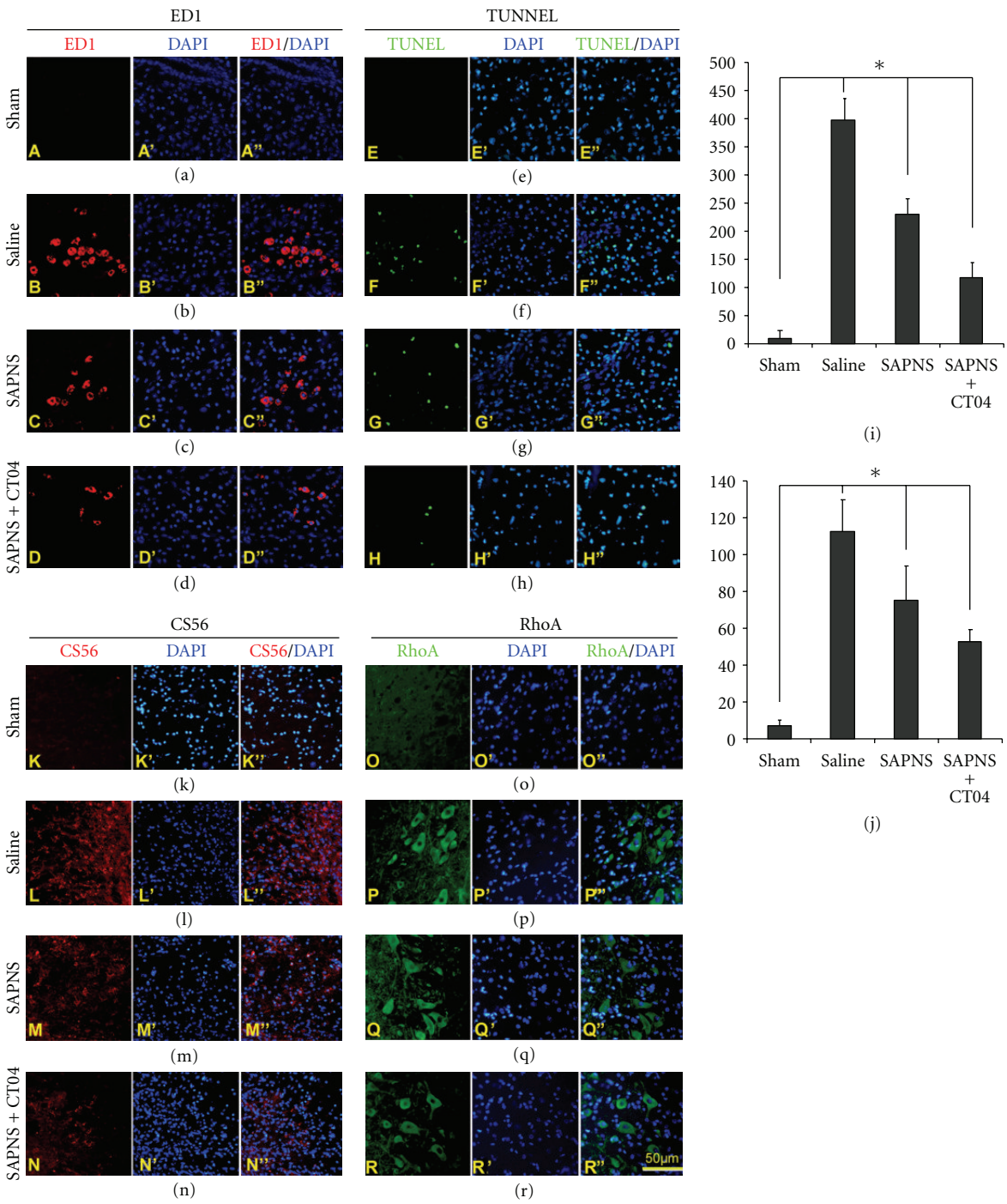

Figure 5: Macrophages infiltration, apoptosis, glial scarring, and RhoA expression 1 wk after treatments. (A–D) show that ED1-positive macrophages surround the lesion site; (E–H) show TUNEL-positive apoptosis cells surround the lesion site; (i, j) show the quantification of ED1-positive macrophages (I) and TUNEL-positive apoptosis cells (J). (K–N) show CS56 immunoreactivities surround the lesion site; (O–R) show RhoA-positive cells surround the lesion site. A–H and K–N were taken in the rostral spinal cord 50 μm from the lesion site. O–R were taken in the 200 μm rostral from the lesion site. Scale bar is 50 μm for all images.

permeable RhoA inhibitor which of the active site is C3 transferase, CT04 released from the mixture implant significantly improved the therapeutic outcomes. Moreover, macrophage infiltration and apoptosis were reduced significantly in the injured spinal cord with combination therapy compared to the controls. Collectively, our results indicated that SAPNS enhanced with delivery of RhoA inhibitor CT04 represented a highly promising therapeutic strategy for SCI via reknitting lesion gap, attenuating secondary injury, and improving axonal regrowth.

Acknowledgments

Funding supports were provided by the Southern Medical University (no. C1010087) and National Natural Science Foundation of China (NSFC, no. 30973095) to J. Guo and the Spinal Cord Injury Foundation of the University of Hong Kong and National Basic Research Program of China (973 program, 2011CB504402) to W. Wu.

References

[1] P. J. Horner and F. H. Gage, "Regenerating the damaged central nervous system," *Nature*, vol. 407, no. 6807, pp. 963–970, 2000.

[2] J. R. Siebert and D. J. Osterhout, "The inhibitory effects of chondroitin sulfate proteoglycans on oligodendrocytes," *Journal of Neurochemistry*, vol. 119, no. 1, pp. 17–188, 2011.

[3] J. K. Lee and B. Zheng, "Role of myelin-associated inhibitors in axonal repair after spinal cord injury," *Experimental Neurology*, vol. 235, no. 1, pp. 33–42, 2012.

[4] S. C. Jefferson, N. J. Tester, and D. R. Howland, "Chondroitinase ABC promotes recovery of adaptive limb movements and enhances axonal growth caudal to a spinal hemisection," *Journal of Neuroscience*, vol. 31, no. 15, pp. 5710–5720, 2011.

[5] B. Zörner and M. E. Schwab, "Anti-Nogo on the go: from animal models to a clinical trial," *Annals of the New York Academy of Sciences*, vol. 1198, no. 1, pp. E22–E34, 2010.

[6] Y. Cao, J. S. Shumsky, M. A. Sabol et al., "Nogo-66 receptor antagonist peptide (NEP1-40) administration promotes functional recovery and axonal growth after lateral funiculus injury in the adult rat," *Neurorehabilitation and Neural Repair*, vol. 22, no. 3, pp. 262–278, 2008.

[7] J. Dill, A. R. Patel, X. L. Yang, R. Bachoo, C. M. Powell, and S. Li, "A molecular mechanism for ibuprofen-mediated RhoA inhibition in neurons," *Journal of Neuroscience*, vol. 30, no. 3, pp. 963–972, 2010.

[8] M. K. Erschbamer, C. P. Hofstetter, and L. Olson, "RhoA, RhoB, RhoC, Rac1, Cdc42, and Tc10 mRNA levels in spinal cord, sensory ganglia, and corticospinal tract neurons and long-lasting specific changes following spinal cord injury," *Journal of Comparative Neurology*, vol. 484, no. 2, pp. 224–233, 2005.

[9] J. K. Sung, L. Miao, J. W. Calvert, L. Huang, H. L. Harkey, and J. H. Zhang, "A possible role of RhoA/Rho-kinase in experimental spinal cord injury in rat," *Brain Research*, vol. 959, no. 1, pp. 29–38, 2003.

[10] P. Duffy, A. Schmandke, A. Schmandke et al., "Rho-associated kinase II (ROCKII) limits axonal growth after trauma within the adult mouse spinal cord," *Journal of Neuroscience*, vol. 29, no. 48, pp. 15266–15276, 2009.

[11] T. Kubo and T. Yamashita, "Rho-ROCK inhibitors for the treatment of CNS injury," *Recent Patents on CNS Drug Discovery*, vol. 2, no. 3, pp. 173–179, 2007.

[12] B. Xing, H. Li, H. Wang et al., "RhoA-inhibiting NSAIDs promote axonal myelination after spinal cord injury," *Experimental Neurology*, vol. 231, no. 2, pp. 247–260, 2011.

[13] L. McKerracher and H. Higuchi, "Targeting Rho to stimulate repair after spinal cord injury," *Journal of Neurotrauma*, vol. 23, no. 3-4, pp. 309–317, 2006.

[14] S. Lord-Fontaine, F. Yang, Q. Diep et al., "Local inhibition of Rho signaling by cell-permeable recombinant protein BA-210 prevents secondary damage and promotes functional recovery following acute spinal cord injury," *Journal of Neurotrauma*, vol. 25, no. 11, pp. 1309–1322, 2008.

[15] M. Hara, M. Takayasu, K. Watanabe et al., "Protein kinase inhibition by fasudil hydrochloride promotes neurological recovery after spinal cord injury in rats," *Journal of Neurosurgery*, vol. 93, no. 1, pp. 94–101, 2000.

[16] A. E. Fournier, B. T. Takizawa, and S. M. Strittmatter, "Rho kinase inhibition enhances axonal regeneration in the injured CNS," *Journal of Neuroscience*, vol. 23, no. 4, pp. 1416–1423, 2003.

[17] S. Otsuka, C. Adamson, V. Sankar et al., "Delayed intrathecal delivery of RhoA siRNA to the contused spinal cord inhibits allodynia, preserves white matter, and increases serotonergic fiber growth," *Journal of Neurotrauma*, vol. 28, no. 6, pp. 1063–1076, 2011.

[18] C. I. Dubreuil, M. J. Winton, and L. McKerracher, "Rho activation patterns after spinal cord injury and the role of activated Rho in apoptosis in the central nervous system," *Journal of Cell Biology*, vol. 162, no. 2, pp. 233–243, 2003.

[19] J. Guo, H. Su, Y. Zeng et al., "Reknitting the injured spinal cord by self-assembling peptide nanofiber scaffold," *Nanomedicine*, vol. 3, no. 4, pp. 311–321, 2007.

[20] J. Guo, K. K. G. Leung, H. Su et al., "Self-assembling peptide nanofiber scaffold promotes the reconstruction of acutely injured brain," *Nanomedicine*, vol. 5, no. 3, pp. 345–351, 2009.

[21] S. Koutsopouios, L. D. Unsworth, Y. Nagai, and S. Zhang, "Controlled release of functional proteins through designer self-assembling peptide nanofiber hydrogel scaffold," *Proceedings of the National Academy of Sciences of the United States of America*, vol. 106, no. 12, pp. 4623–4628, 2009.

[22] Y. Nagai, L. D. Unsworth, S. Koutsopoulos, and S. Zhang, "Slow release of molecules in self-assembling peptide nanofiber scaffold," *Journal of Controlled Release*, vol. 115, no. 1, pp. 18–25, 2006.

[23] R. E. Miller, P. W. Kopesky, and A. J. Grodzinsky, "Growth fac textbfa-tor delivery through self-assembling peptide scaffolds," *Clinical Orthopaedics and Related Research*, vol. 469, no. 10, pp. 2716–2724, 2011.

[24] F. Li, J. Wang, F. Tang et al., "Fluorescence studies on a designed self-assembling peptide of RAD16-ll as a potential carrier for hydrophobic drug," *Journal of Nanoscience and Nanotechnology*, vol. 9, no. 2, pp. 1611–1614, 2009.

[25] J. Liu, L. Zhang, Z. Yang, and X. Zhao, "Controlled release of paclitaxel from a self-assembling peptide hydrogel formed in situ and antitumor study in vitro," *International Journal of Nanomedicine*, vol. 6, pp. 2143–2153, 2011.

[26] J. Guo, K. K. G. Leung, and W. Wu, "Nanofiber scaffold and injured nervous system," in *Nanomedicine and the Nervous System*, pp. 330–346, Science Publishers, 2012.

[27] H. A. Benink and W. M. Bement, "Concentric zones of active RhoA and Cdc42 around single cell wounds," *Journal of Cell Biology*, vol. 168, no. 3, pp. 429–439, 2005.

[28] S. Zhang, "Designer self-assembling Peptide nanofiber scaffolds for study of 3-d cell biology and beyond," *Advances in Cancer Research*, vol. 99, pp. 335–362, 2008.

[29] T. Kamada, M. Koda, M. Dezawa et al., "Transplantation of bone marrow stromal cell-derived Schwann cells promotes axonal regeneration and functional recovery after complete transection of adult rat spinal cord," *Journal of Neuropathology and Experimental Neurology*, vol. 64, no. 1, pp. 37–45, 2005.

[30] J. S. Guo, Y. S. Zeng, H. B. Li et al., "Cotransplant of neural stem cells and NT-3 gene modified Schwann cells promote the

recovery of transected spinal cord injury," *Spinal Cord*, vol. 45, no. 1, pp. 15–24, 2007.

[31] D. M. Basso, L. C. Fisher, A. J. Anderson, L. B. Jakeman, D. M. McTigue, and P. G. Popovich, "Basso mouse scale for locomotion detects differences in recovery after spinal cord injury in five common mouse strains," *Journal of Neurotrauma*, vol. 23, no. 5, pp. 635–659, 2006.

[32] H. M. Geller and J. W. Fawcett, "Building a bridge: engineering spinal cord repair," *Experimental Neurology*, vol. 174, no. 2, pp. 125–136, 2002.

[33] C. A. E. Hauser and S. Zhang, "Designer self-assembling peptide nanofiber biological materials," *Chemical Society Reviews*, vol. 39, no. 8, pp. 2780–2790, 2010.

[34] R. G. Ellis-Behnke, Y. X. Liang, D. K. C. Tay et al., "Nano hemostat solution: immediate hemostasis at the nanoscale," *Nanomedicine*, vol. 2, no. 4, pp. 207–215, 2006.

[35] S. Etienne-Manneville and A. Hall, "Rho GTPases in cell biology," *Nature*, vol. 420, no. 6916, pp. 629–635, 2002.

[36] B. J. Dickson, "Molecular mechanisms of axon guidance," *Science*, vol. 298, no. 5600, pp. 1959–1964, 2002.

[37] S. Yamagishi, M. Fujitani, K. Hata et al., "Wallerian degeneration involves Rho/Rho-kinase signaling," *Journal of Biological Chemistry*, vol. 280, no. 21, pp. 20384–20388, 2005.

[38] A. J. Ridley, "Rho proteins, PI 3-kinases, and monocyte/macrophage motility," *FEBS Letters*, vol. 498, no. 2-3, pp. 168–171, 2001.